Photochemical Studies of Hydrogen Peroxide in Solid Rare Gases: Formation of the HOH···O(^{3}P) Complex

Susanna Pehkonen,* Mika Pettersson, Jan Lundell, Leonid Khriachtchev, and Markku Räsänen

Laboratory of Physical Chemistry, University of Helsinki, P.O. Box 55, FIN-00014 University of Helsinki, Finland

Received: May 5, 1998; In Final Form: July 1, 1998

UV photolysis of H_2O_2 in solid Ar, Kr, and Xe yields isolated OH radicals and a complex between a water molecule and a ground-state (^{3}P) oxygen atom. The vibrational bands of the HOH···O complex are observed at 3730.1 and 3633.0 cm^{-1} in Ar, at 3718.6 and 3622.4 cm^{-1} in Kr, and at 3704.3 and 3607.3 cm^{-1} in Xe matrices. The assignment is based on isotopic substitution, selective photoinduced processes between H_2O_2 and HOH···O, and ab initio calculations. In Kr and Xe matrices, the complex is formed with much less efficiency when compared with Ar matrices, indicating the existence of other photolysis channels. Computational results on the complex geometry and vibrational frequencies are presented and compared with experimental data.

1. Introduction

Hydrogen peroxide has, besides industrial uses, a great significance in atmospheric oxidation reactions[1] and combustion chemistry,[2] and it has also been a subject of numerous photodissociation dynamics studies.[3] Also, many biochemical reactions involve the formation of H_2O_2, for example, the production of halogenated organic compounds in seawater by haloperoxidase.[4]

In principle, a number of possible photodissociation channels of H_2O_2 can be written. In 193 nm photolysis, the following reactions are energetically possible:

$$H_2O_2 \rightarrow H + OOH \quad (1)$$

$$H_2O_2 \rightarrow H_2O + O(^1D) \quad (2)$$

$$H_2O_2 \rightarrow 2OH(X^2\Pi) \quad (3)$$

$$H_2O_2 \rightarrow H_2OO \quad (4)$$

$$H_2O_2 \rightarrow H_2O + O(^3P) \quad (5)$$

$$H_2O_2 \rightarrow H_2 + O_2 \quad (6)$$

The photodissociation product in reaction 4 is the hypothetical oxywater, where an oxygen atom in a water molecule forms a bond to another oxygen atom. Oxywater was theoretically predicted to exist[5−8] and indirectly detected by mass spectroscopy.[9]

In the gas phase, photodissociation of hydrogen peroxide has been studied extensively.[10−20] The experiments have shown that the main primary product in UV photolysis above 172.2 nm are two ground-state OH radicals.[10,14] The two OH radicals can react to give water and atomic oxygen.[18]

$$OH + OH \rightarrow H_2O + O \quad (7)$$

Photodissociation of H_2O_2 at 248 and 193 nm yields largely vibrationless OH radicals with a very narrow rotational-state distribution. About 90% of the available excess energy is converted to translational energy of the OH radicals.[11,15] Schiffman et al.[19] estimated the quantum yield of OH production (reaction 3) to be 1.22 ± 0.13 in 193 nm photolysis and and 1.58 ± 0.23 in 248 nm photolysis. The low quantum yield, less than two, indicates that there are other photolysis channels. Nevertheless, these additional channels have not been identified yet. For instance, Bohn and Zetzsch estimated the quantum yield for the reaction 1 to be less than 0.05 in 248 nm photolysis.[20]

In solid rare gases, the information on photodissociation of H_2O_2 is less extensive. Kuo et al. [21] studied the photolysis products of hydrogen peroxide in argon matrices in connection with a reaction between hydrogen peroxide and ethene. They reported several new IR bands from the 248 nm photolysis of H_2O_2 and suggested them to be due to water, OH radicals, and their complexes without detailed assignments.

A number of different assignments for IR absorptions of OH radicals can be found in the literature.[21−27] In Ar matrices, they are at about 3452 and 3428 cm^{-1} [24,25] and at 3548.20 cm^{-1}.[26] The luminescence spectra of OH radicals were reported in different rare-gas matrices.[27]

A main question in UV photolysis of H_2O_2 in solid rare-gas environment is what happens in the cage to the primary OH radical pair. There are basically two possibilities: one or both OH radicals can escape from the cage, creating isolated OH radicals, or they can react in the cage. As we have measured recently,[28] the cage-exit probability for an OH radical in 193/248 nm photolysis of H_2O_2 is about 17% in Ar at 17 K. The rest of OH radicals seem to form H_2O + O, resulting in a complex in the cage. In this paper, we identify and characterize the formation of the HOH···O complex by means of IR

* Corresponding author. e-mail susanna.pehkonen@csc.fi.

S1089-5639(98)02111-2 CCC: $15.00
Published on Web 09/09/1998

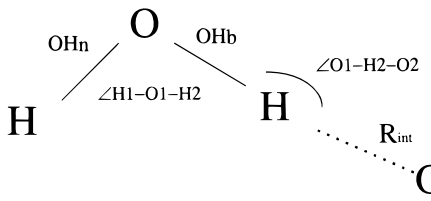

Figure 1. The optimized structure of the planar HOH···O complex.

spectroscopy and ab initio calculations. Different rare-gas solids (Ar, Kr, and Xe) are considered and compared from the viewpoint of the photolysis products.

2. Calculations

2a. Computational Details. All the calculations were performed with the GAUSSIAN94 package[29] using second-order perturbation theory (UMP2). All electrons were included in the correlation calculation. The potential energy surface of HOH···O was preliminarily scanned at the UMP2/6-31G(d,p) level. The found minima were thereafter studied using a larger and more flexible 6-311++G(2d,2p) basis set. This level of calculation was found as an acceptable compromise between efficiency and accuracy for weak chemical interactions.[30] The harmonic vibrational frequencies were calculated analytically.

The interaction energy of the HOH···O complex was evaluated as the difference of total energy between the complex and the monomers at infinite distance, where the monomer wave functions were derived in the dimer-centered basis set. This approach corresponds to the counterpoise correction proposed by Boys and Bernardi[31] aimed to minimize the basis set superposition error (BSSE) in the interaction energy, E_{MP2-CP}.

All the calculations were carried out on SGI Power Challenge and CRAY C94 supercomputers at the CSC-Center for Scientific Computing Ltd. (Espoo, Finland).

2b. Computational Results. A schematic picture of the HOH···O complex is presented in Figure 1. The calculated geometries, electronic energies, and BSSE-corrected interaction energies at various levels of theory are collected in Table 1.

At all levels of theory, the complexed OH bond is elongated compared with the other OH bond. At the smallest level (UMP2/6-311++G(d)) the calculated elongation is only 0.0009 Å, but it increases with the size of the basis set. At the largest UMP2/6-311++G(3d,3p) level, the difference between the complexed and noncomplexed OH bond length is 0.0022 Å.

The effect of complexation on the O(^{3}P) in the water angle appears quite weak, the angle increasing from the monomer value of 104.3°[32] to 105.0° for the complex at the MP2/6-311++G(2d,2p) level. Also, the increase of the basis set has a small effect in the water angle within the complex. On the other hand, increasing the basis set influences strongly on the resulting intermolecular angle $O_1-H_b-O_2$. Using the smallest basis set (6-311++G(d)) the tilt from linearity is ca. 27°, and it decreases with increasing basis set. At the UMP2/6-311++G-(3d,3p) level, the tilt diminishes to 10°, which is very close to the tilt found in HOH···CO complex both computationally[30,33] and experimentally.[34] Other similarities between the perturbation in HOH···O and HOH···CO can also be found. The interaction distance in HOH···O was found to be 2.23 Å at the MP2/6-311++G(2d,2p) level of theory. For HOH···CO the predicted intermolecular distance was slightly longer (2.34 Å) at the same level.[32] The calculated BSSE-corrected interaction energy for HOH···CO at the same level of theory was −6.89 kJ mol^{-1}, which is quite close to the predicted interaction energy for HOH···O (−5.26 kJ mol^{-1}).

The true PES consists of a double minimum where the oxygen can reside at either hydrogen. A crude scan of the PES between these two equal minima at the UMP2/6-311++G(2d,2p) level of theory gives an estimate of 4.7 kJ mol^{-1} for the dividing barrier, which is similar to the interaction energy.

The calculated (scaled by 0.95) harmonic wavenumbers of the HOH···O complex and its deuterated analogues are collected in Table 2. The predicted vibrational shifts of the HOH···O complex are interesting to compare with those of HOH···CO. For the HOH···CO complex, the symmetric and antisymmetric OH stretches were predicted to shift downward (−13.9 and −18.2 cm^{-1}, respectively, at the MP2/6-311++G(2d,2p) level).[32] In Ar matrices, these shifts were observed to be −9.5 and −8.8 cm^{-1}, respectively.[35] For HOH···O the respective shifts are predicted to be −16 and −18 cm^{-1}. Moreover, for the HOH···CO complex the water bending is predicted to shift 11.7 cm^{-1} upward from the monomer value, and experimentally this was confirmed to be +5.4 cm^{-1}.[32] In fact, it is typical for hydrogen-bonded complexes that bending modes associated with the complexation show a shift upward compared with the unperturbed monomer.[36] However, for the HOH···O complex the predicted shift is downward by ∼5 cm^{-1}.

3. Experiments

3a. Experimental Setup. Hydrogen peroxide was obtained from commercially available urea hydrogen peroxide (Aldrich, 98% nominal purity) as described elsewhere.[37] Deuterated urea hydrogen peroxide was synthesized from urea, deuterated water, and 30% hydrogen peroxide solution.[38] Argon (99.9999% purity, AGA), krypton, and xenon (99.997% purity, CF_4 free, AGA) were used without further purification. The gas mixture was deposited on a CsI or KBr window typically at 17 K. A closed cycle helium refrigerator (Air Product's Displex DE-202A) was used for cooling. The matrix can be heated with a resistive heater, and the temperature was measured with a silicon diode attached onto the frame of the cold window.

An excimer laser (ELI-76, Estonian Academy of Sciences) was used for photolysis experiments at wavelengths 193 nm (ArF) and 248 nm (KrF). The energy of the laser pulse at the sample (diameter 20 mm) was typically 5−20 mJ. In some experiments frequency-doubled radiation from an optical parametric oscillator (Continuum, OPO Sunlite), tunable down to 225 nm, was also used. The infrared spectra were recorded with a Nicolet 60 SX FTIR spectrometer in the region of 4000−400 cm^{-1} coadding 200 scans. Resolution used in the experiments was 1 or 0.25 cm^{-1}. Luminescence was analyzed with a single UV−vis monochromator (Spex 270 M, resolution 0.3 nm) equipped with a gated ICCD camera (Princeton Instruments, time resolution down to 3 ns). With a deposition line made from PFA-plastic (Swagelock), the decomposition of hydrogen peroxide to water and oxygen could be minimized, although weak absorptions of monomeric water were seen in the IR spectra.

3b. Experimental Results: Ar Matrices. The IR spectrum of hydrogen peroxide in Ar, Kr, and Xe matrices has been analyzed elsewhere.[37,39] In solid Ar, the OH stretching fundamentals of H_2O_2 lie at 3597.8 and 3587.8 cm^{-1} and the antisymmetric bending is at 1270.9 and 1277.0 cm^{-1}.[37] Monomeric water absorptions, in agreement with the literature data, were observed as an impurity. The absorptions of H_2O_2 in solid Kr and Xe are very similar, shifted a few wavenumbers downward from the values in solid Ar.[37]

Figure 2 presents a result of 193 nm photolysis of H_2O_2 in solid Ar. The negative signals correspond to the decomposition

TABLE 1: Optimized Geometries, Electronic Energies, and Interaction Energies of the Planar HOH···O Complex[a]

	OH_n (Å)	OH_b (Å)	R_{int} (Å)	∠H1−O1−H2 (deg)	∠O1−H2−O2 (deg)	E_{el} (hartrees)	E_{MP2-CP} (kJ mol^{-1})
UMP2/6-311++G(d)	0.9591	0.9600	2.3178	107.8	153.3	−151.169 449 0	−4.437
UMP2/6-311++G(d,p)	0.9591	0.9604	2.3150	103.8	164.1	−151.199 257 7	−4.544
UMP2/6-311++G(2d)	0.9626	0.9640	2.2903	105.4	156.4	−151.209 806 3	−5.125
UMP2/6-311++G(3d)	0.9628	0.9646	2.2455	104.4	165.2	−151.219 187 4	−5.561
UMP2/6-311++G(2d,p)	0.9622	0.9639	2.2763	105.0	161.1	−151.227 961 1	−5.287
UMP2/6-311++G(2d,2p)	0.9522	0.9544	2.2324	105.0	167.7	−151. 234 328 9	−5.260
UMP2/6-311++G(3d,p)	0.9621	0.9641	2.2389	105.0	164.2	−151. 235 546 1	−5.740
UMP2/6-311++G(3d,2p)	0.9582	0.9604	2.2072	104.8	166.0	−151. 239 501 6	−5.691
UMP2/6-311++G(3d,3p)	0.9587	0.9609	2.2085	104.8	170.0	−151. 240 507 8	−5.602

[a] The letter n refers to nonbonded and b to bonded OH.

TABLE 2: Calculated and Experimental Vibrational Frequencies (in cm^{-1}) and Estimated Vibrational Shifts upon Formation of the HOH···O Complex

complex form	water−oxygen complex		water molecule		freq shift	
	calcd[a]	exptl	calcd[a]	exptl[b]	theortl	exptl
HO**H**···O	3773 (129)	3730 (100)	3790 (74)	3734.3	−16	−4
	3658 (52)	3633 (33)	3676 (10)	3638.0	−18	−5
	1572 (57)		1578 (66)	1589.1	−5	
	229 (83)					
	159 (98)					
	100 (6)					
HO**D**···O	3739 (46)	3700 (36)	3734 (47)	3687.3	5	13
	2691 (74)	2692 (100)	2710 (21)	2710.0	−19	−18
	1374 (50)		1383 (57)	1398.8	−10	
	171 (29)					
	136 (62)					
	100 (10)					
DO**H**···O	3708 (153)	3665	3734 (47)	3687.3	−26	−22
	2714 (18)		2710 (21)	2710.0	4	
	1385 (53)		1383 (57)	1398.8	2	
	234 (104)					
	141 (63)					
	102 (7)					
DO**D**···O	2769 (79)	2767 (100)	2777 (45)	2771.1	−8	−4
	2641 (27)	2653 (24)	2649 (7)	2657.7	−8	−5
	1150 (31)		1155 (35)	1174.6	−5	
	177 (47)					
	119 (38)					
	98 (15)					

[a] The UMP2/6-311++G(2d,2p) level of theory was used for calculations. The calculated frequencies are scaled with a scale factor of 0.95. The numbers in parentheses are the relative infrared intensities given in units of km mol^{-1}. [b]Reference 40.

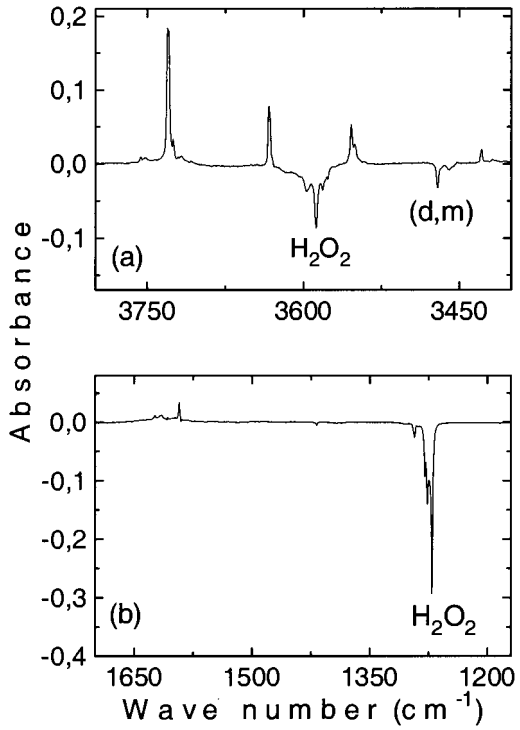

Figure 2. A differential spectrum of the photolysis products in solid Ar at 17 K: panel a, OH stretching region; panel b, OH bending region. The negative peaks indicate monomeric (H_2O_2) and dimer or multimeric (d, m) bands of H_2O_2.

of H_2O_2, and several new IR absorptions appear. The sharp bands at 3730.1 and 3633.0 cm^{-1} belong to the same absorber, and the band at 3554.1 cm^{-1} belongs to another species, which can be seen by comparing the correlation between the IR bands at different stages of the photolysis. Also, irradiation of the matrix generates weaker absorptions at wavenumbers 3725.4 (shoulder), 3452, 3428.6, 1630 (broad), and 1592.9 cm^{-1}. Ozone (1039 cm^{-1}) is detected in very small amounts after prolonged photolysis with the excimer laser. All the strongest IR bands with the appropriate assignments to the photolysis products are listed in Table 3.

UV photolysis of deuterated samples is presented in Figures 3 and 4. Upon deuteration, the 3730.1 and 3633.0 cm^{-1} lines shift to 2766.5 and 2653 cm^{-1}, and also a strong band at 2691.8 cm^{-1} and two weaker bands at 3699.8 and 3664.9 cm^{-1} grow in photolysis. In the photolysis experiments where DOOH and HOOH dominated as precursors, irradiation produces only one OD stretching at 2691.8 cm^{-1}, as indicated in Figure 5. The 3554.1 cm^{-1} peak and its shoulder at 3550.2 cm^{-1} shift to 2620.1 and 2617.3 cm^{-1}. The IR bands of the photolysis products from D_2O_2 and HDO_2 are also listed in Table 3.

When the IR spectrum was recorded at higher resolution of 0.25 cm^{-1}, a doublet structure in the absorption bands was observed, as seen Figure 6. The doublet structure is visible in all isotope-substituted species. In experiments with H_2O_2, the doublets are at 3730.7 and 3729.3 cm^{-1} and at 3633.5 and 3632.3 cm^{-1}. Upon deuteration, the following doublets are formed: 2767.0 and 2766.2 cm^{-1}, 2692.1 and 2691.2 cm^{-1}, 3699.8 and 3698.6 cm^{-1}, and 3664.8 and 3663.7 cm^{-1}. We suggest that the splitting is due to site effects.

When a photolyzed matrix is annealed, the complex starts to decompose. The growth of monomeric water and ozone is detected after annealing above 25 K. The formation of water indicates that the complex consists of complexed water. The ozone is due to the reaction of oxygen atoms with each other or with impurity oxygen molecule.

4. Assignment and Discussion: Ar Matrices

Comparison of the 3730.1 and 3633.0 cm^{-1} lines with the unperturbed monomeric water band centers in an Ar matrix (3734.3 and 3638.0 cm^{-1} for ν_3 and ν_1, respectively)[40] suggests strongly that these bands originate from complexed water

TABLE 3: Strongest Photolysis Products of H_2O_2 in Ar, Kr, and Xe Matrices[a]

Ar	Kr	Xe	assignt
	3747.5		H_2O
3730.1	3718.6	3704.3	HO**H**···**O** ν_3
3699.8			HO**D**···**O**
3664.9			DO**H**···**O**
		3695.8	H_2O
3633.2	3622.4	3607.3	HO**H**···**O** ν_1
3554.1	3547.1	3530	OH
3550.2	3541.8		OH
	3538.6		OH
	3414.4	3401.8	HOO (free or complexed)
2766.5	2758.8	2749.1	DO**D**···**O** ν_3
2691.8	2689.5		HO**D**···**O**
2653		2674.8	DO**D**···**O** ν_1
2620.1	2615.9		OD
2617.3	2613.5		OD
1630 broad			δ_{HOH}?
1592.9	1589.9	1586.7	δ_{HOH}?
		1383.9	HOO (free or complexed)
1174	1172		
		1095	HOO (free or complexed)

[a] In the complex formation, atoms connected with dots indicate the complex bond.

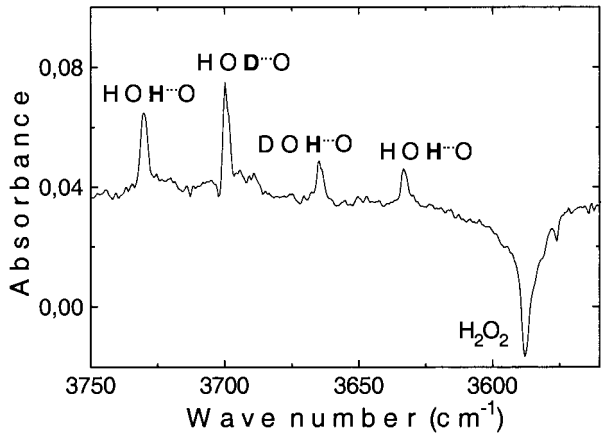

Figure 3. A differential spectrum of the photolysis products in the ν_{OH} region in Ar at 17 K, when D_2O_2, HDO_2, and H_2O_2 is present.

molecules. The corresponding bands of deuterated species are shifted from monomeric bands of D_2O (2771.1 and 2657.7 cm^{-1} for ν_3 and ν_1 in Ar, respectively) and HDO (2710.0 and 3687.3 cm^{-1} for ν_1 and ν_3 in Ar, respectively).[40] It is clear that there is only one possible water complex arising from the photolysis of monomeric H_2O_2, HOH···O. The appearance of this complex agrees with photochemistry of H_2O_2 known for the gas phase (see reactions 3 and 7), and this complex was computationally shown above to be energetically stable. Also, the absorptions growing in the photolysis correspond well to the calculated vibrational frequencies of the HOH···O. Water dimer as a photolysis product can be excluded, because their absorptions are known to be different from those observed in our study.[40]

Thus, we assign the lines at 3730.1 and 3633.0 cm^{-1} to ν_3 and ν_1 modes of the complex, HO**H**···O, and the lines at 2766.5 and 2653 cm^{-1} belong to ν_3 and ν_1 of DO**D**···O. The isotopic shifts are 1.348 and 1.369 for ν_3 and ν_1, respectively, and they are very close to the isotopic shifts of monomeric water in Ar.[40] The difference between the two OH stretchings of the HDO complex, 34.9 cm^{-1}, exceeds site effects, and we propose that

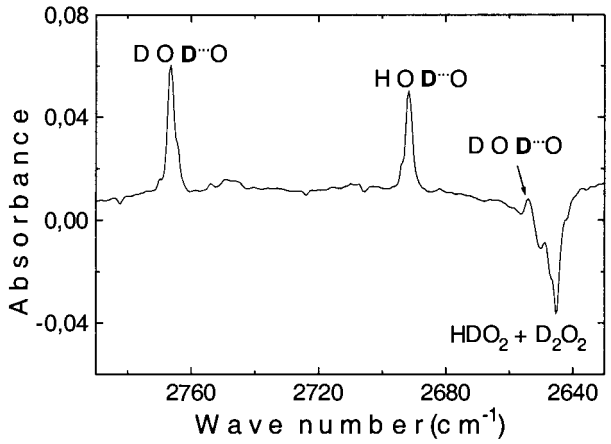

Figure 4. A differential spectrum of the photolysis products in the ν_{OD} region in Ar, when D_2O_2, HDO_2, and a very small amount of H_2O_2 are present.

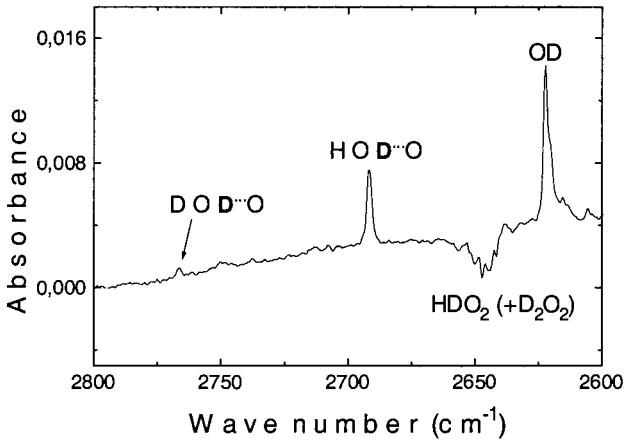

Figure 5. A differential spectrum of the photolysis products in the ν_{OD} region in Ar, when HDO_2 and H_2O_2 are present. The negative peaks belong to photolyzed HDO_2 and to a very small amount of D_2O_2.

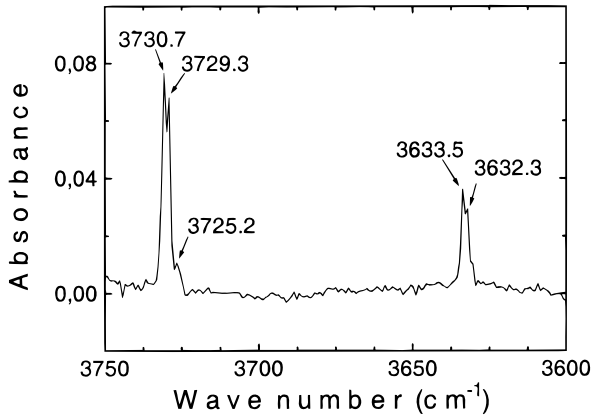

Figure 6. ν_{OH} absorption of HOH···O complex measured at 0.25 cm^{-1} resolution in Ar at 17 K.

these bands arise from two isomers, H-bonded and D-bonded forms, of HDO···O complexes. In many water complexes, HDO prefers the interaction via the deuterium atom,[41] and the stronger bands at 3699.8 and 2691.8 cm^{-1} are assigned to OH and OD stretchings of a HOD···O complex. The OH stretching of the DO**H**···**O** is observed at 3664.9 cm^{-1}. Computationally, the OD stretching of the DO**H**···O complex lies at about 2714 cm^{-1}, and it appears much weaker than the corresponding band in HO**D**···O. This may be the reason why we do not observe it.

Bending absorptions of the HOH···O complex and the corresponding deuterated species were not identified, and there can be at least two reasons for this. First, the absorptions can overlap with some water impurity bands, and second, the absorption can be difficult to identify if the band is broadened and locates in the water absorption region. In the bending region, we observe a very broad absorption at 1630 cm^{-1} (fwhm 62 cm^{-1}), and it seems to correlate with the OH stretchings of the HOH···O complex. However, the experimental shift from the monomeric water is 41 cm^{-1} compared with calculated shift of −5 cm^{-1}. The bending mode of the HOH···O complex can also be hidden under the 1592 cm^{-1} absorption, which is very close to calculations of the HOH···O bending mode. It should be mentioned that Engdahl and Nelander also failed to observe the water bending absorptions in the water−iodine complex.[42]

As an additional support of our assignments, it can be noticed that the vibrational properties of the HOH···O complex are very similar to those of the water−iodine complex studied by Engdahl and Nelander.[42] The HOH···I complex ν_3 and ν_1 fundamentals are at 3714.3 and 3617.0 cm^{-1}, and they show a doublet structure below 17 K. According to the authors, the bending motion of water−iodine complex can be hidden under the rotational structure of free water or other water absorptions, which is also similar to the present case.

Further evidence for the formation of the HOH···O complex can be found in photochemical studies on H_2O_2. In our previous paper,[28] we showed that H_2O_2 can be recovered from its photolysis products by a photoinduced reaction, and the HOH···O complex was suggested to be the starting structure of the reaction. It was also shown that the normalized sum of H_2O_2, HOH···O, and OH radical pair remained unity during the irradiation process, which indicates the closeness of the photochemical scheme

$$\mathrm{HOH\cdots O} \leftrightarrow \mathrm{H_2O_2} \rightarrow \mathrm{2OH} \qquad (8)$$

The most efficient production of the HOH···O complex (up to 55%) was obtained with the shortest wavelength 193 nm from the excimer laser. Irradiation at longer wavelengths, for example at 300 nm, after 193 nm generation of HOH···O, restored hydrogen peroxide, which can be described by the scheme

$$\mathrm{H_2O_2} \xrightarrow{193\ \mathrm{nm}} \mathrm{HOH\cdots O} \xrightarrow{300\ \mathrm{nm}} \mathrm{H_2O_2} \qquad (9)$$

This process is illustrated in Figure 7. First, photolysis of H_2O_2 dominates the photorecovery at 193 nm. Under irradiation at longer wavelengths (here 300 nm), the photorecovery of H_2O_2 becomes much more efficient than H_2O_2 decomposition. The amount of OH radicals does not change during the 300 nm irradiation. This photorecovery reaction verifies the production of the HOH···O complex in the photolysis of H_2O_2. Indeed, the photorecovery of monomeric H_2O_2 proves that the complex consists of two hydrogen atoms and two oxygen atoms, and we can suggest only one candidate for this structure, HOH··· O. The details of the photochemistry on H_2O_2 can be found elsewhere.[28]

On the basis of simultaneous luminescence measurements, we assigned the OH radical in Ar at 3554.1 cm^{-1} (with a shoulder at 3550.2 cm^{-1}),[28] our corresponding OD values being 2620.1 and 2617.3 cm^{-1}. With this assignment, also the ν_{OH}/ν_{OD} ratio 1.356 is quite close to the gas-phase value.

Now, we discuss the possibility of other dissociation channels for H_2O_2. A reaction channel producing hydrogen and oxygen molecules can be discarded because we have shown by luminescence measurements that molecular oxygen is not formed in the photolysis of monomeric H_2O_2 in solid Ar.[28] Small amounts of ozone in the matrix can be formed possibly from impurity O_2 molecules. Dissociation of monomeric H_2O_2 to hydroperoxyl radical, HOO, and hydrogen atom is also possible. However, no sign of HOO radicals, which are known to absorb at 3412.5, 1388.5, and 1101.1 cm^{-1},[43] was observed in the infrared spectra after UV photolysis of H_2O_2 in argon matrix. Photolysis of dimeric (or multimeric) H_2O_2 should produce the HOO−HOH complex reported by Nelander,[44] and it was observed in our experiments in 275−300 nm photolysis in very concentrated H_2O_2/Ar matrices. The formation of oxywater as a stable photolysis product in the photolysis of H_2O_2 can also be excluded. According to theoretical calculations on H_2OO by Huang et al.,[6] the intensity of the O−O stretching vibration (666 cm^{-1}, intensity 113 km mol^{-1}) should be similar to that of OH stretching. However, our experiments in argon show no sign of O−O stretching that would indicate the presence of oxywater. Even if the O−O stretching were too weak to be observed, the absorptions assigned in this work cannot belong to oxywater, because the partly deuterated oxywater, HDO−O, would have single OH and OD stretching bands, but we observe two OH stretchings assigned to H-bonded and D-bonded forms of the complex, HOD···O and DOH···O. Ozone is also known to form a complex with water,[45] and the fundamentals are at 3726.5, 3632.5, and 1592.5 cm^{-1} and at 2765.5, 2654, and 1176.5 cm^{-1} for the $D_2O\cdots O_3$ complex. These lines do not match with our complex bands at 3730.1 and 3633.0 cm^{-1}, and only the strongest ozone vibration is observed in the infrared spectra after prolonged irradiation by 193 nm.

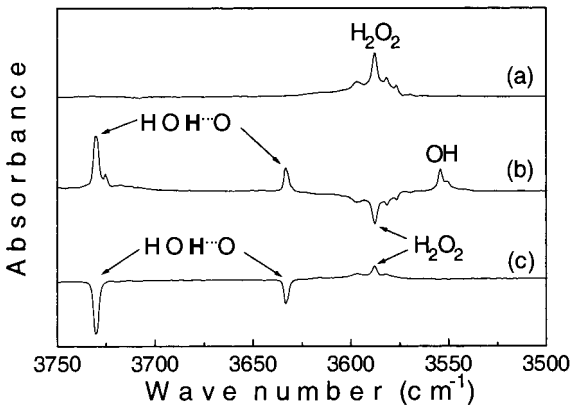

Figure 7. Photolysis scheme of H_2O_2 in argon. (a) A spectrum of H_2O_2 before irradiation. (b) The formation of water−oxygen complex by 193 nm irradiation, a difference spectrum. The negative lines indicate dissociated H_2O_2. (c) A difference spectrum of the decomposition of the water−oxygen complex at 300 nm. Notice that the amount of OH radicals does not change during the decrease of the HOH···O complex.

5. Kr and Xe Matrices

In solid Kr, we observe the OH stretchings of the HOH···O complex at 3718.6 and 3622.4 cm^{-1}. The formation of the complex by 193 or 248 nm is not as efficient as in Ar matrix, and it decomposes easily upon further irradiation. The OH radicals were detected to absorb at 3547.1, 3541.8, and 3538.6 cm^{-1}. Monomeric water absorptions grow in photolysis in Kr, suggesting that oxygen atom escapes from the cage after the reaction OH + OH → H_2O + O. Also, a new sharp line at 3414.4 cm^{-1} appears in photolysis in Kr, and this line does not have a counterpart in Ar. This line is tentatively assigned to free or complexed HOO. The strongest IR absorptions of the photolysis products in Kr and Xe matrices are given in Table 3.

In Xe matrices two lines at 3718.6 and 3622.4 cm^{-1}, belonging to the HOH···O complex, are observed in the IR spectra. OH radicals are detected at 3530 cm^{-1}, but the amount of OH radicals is very small compared to Ar and Kr. Three lines found in Xe at 3401.8 (strongest), 1383.9, and 1095 cm^{-1}, assigned to free or complexed HO_2, suggest other photolysis channels. Weak absorptions due to monomeric water are also observed to grow in photolysis. In the photolysis of deuterated samples, two very weak lines appear at 2749.1 and 2674.8 cm^{-1}, which belong to deuterated complexes.

In Xe matrices, we detect free oxygen atoms after 266−285 nm photolysis by using laser-induced luminescence, as suggested by Lawrence and Apkarian.[46] This and the formation of monomeric water in the photolysis gives evidence of the escape of oxygen atoms from the HOH···O complex. Dissociation to hydroperoxyl radical and hydrogen atom is also a possible channel. The infrared spectrum of HO_2 has not been reported in Xe matrices; however, the absorptions should be similar to those in Ar. Three lines found in Xe at 3401.8, 1383.9, and 1095 cm^{-1} are assigned to free or complexed HO_2. However, there are two possible routes to generate HOO: primary photolysis channel (reaction 1) or secondary mobility assisted reactions. For example, the primary photolysis process can still be the decomposition of H_2O_2 to two OH radicals, which form the HOH···O complex. In the following, the escaping oxygen atom from the HOH···O complex reacts further with OH radical producing HOO:

$$H_2O_2 \rightarrow OH + OH \rightarrow HOH\cdots O \rightarrow H_2O + O \quad (10)$$

$$O + OH \rightarrow HOO \quad (11)$$

This model (10−11) explains the small amount of OH radicals observed in Xe matrices.

6. Conclusions

The complex between a water molecule and a ground-state oxygen atom is one of the products formed in UV photolysis of H_2O_2 in rare-gas matrices. A way to form the HOH···O complex includes primary photodissociation of H_2O_2 into a pair of OH radicals followed by the cage induced reaction between them. The complexation with atomic oxygen shifts the water stretchings downward by 4−5 cm^{-1} with respect to monomeric water. Isotopic substitution and ab initio calculations support the assignments. Also, the photorecovery of monomeric H_2O_2 from this photolysis product suggests the same constitution, HOH···O. The formation of the HOH···O complex is most efficient in Ar, decreases in Kr, and becomes quite minor in Xe matrices, probably indicating an enhancement of secondary processes, cage exit of the oxygen atom, for example.

Acknowledgment. S.P. acknowledges the support of a grant for young scientists from the University of Helsinki. This research was also supported partially by the EU Project LAMOCS, Grant ENV4-CT95-0046. The CSC-Center of Scientific Computing Ltd. (Espoo, Finland) is gratefully thanked for providing the computing facilities.

References and Notes

(1) See for example: Finlayson-Pitts, B. J.; Pitts, J. N., Jr. *Atmospheric Chemistry: Fundamentals and Experimental Techniques*; A Wiley-Interscience Publication; John Wiley & Sons: New York, 1986.

(2) Tsang, W.; Hampson, R. F. *J. Phys. Chem. Ref. Data* **1986**, *15*, 1087.

(3) Schinke, R. *Photodissociation Dynamics*; Cambridge University Press: New York, 1993.

(4) Kankaanpää, H. Sedimentation, distribution, sources and properties of organic material in Gulf of Finland. Dissertation, Monograph of Borealis Environment Research, 1997.

(5) Meredith, C.; Hamilton, T. P.; Schaefer III, H. F. *J. Phys. Chem.* **1992**, *96*, 9250.

(6) Huang, H. H.; Xie, Y.; Schaefer III, H. F. *J. Phys. Chem.* **1996**, *100*, 6076.

(7) Xie, Y. M.; Allen, W. D.; Yamaguchi, Y.; Schaefer III, H. F. *J. Chem. Phys.* **1996**, *100*, 7615.

(8) Jursic, B. S. *J. Mol. Struct. (THEOCHEM)* **1997**, *417*, 81.

(9) Schröder, D.; Schalley, C. A.; Goldberg, N.; Hrusak, J.; Schwarz, H. *J. Chem. Eur.* **1996**, *2*, 1235.

(10) Suto, M.; Lee, L. C. *Chem. Phys. Lett.* **1983**, *98*, 152.

(11) Ondrey, G.; van Veen, N.; Bersohn, R. *J. Chem. Phys.* **1983**, *78*, 3732.

(12) Bersohn, R.; Shapiro, M. *J. Chem. Phys.* **1986,** *85*, 1396.

(13) Klee, S.; Gericke, K.-H.; Comes, F. J. *J. Phys. Chem.* **1986**, *85*, 40.

(14) Docker, M. P.; Hodgson, A.; Simons, J. P. *Chem. Phys. Lett.* **1986**, *128*, 264.

(15) Comes, F. J.; Gericke, K.-H.; Grunevald; A. V.; Klee, S. *Ber. Bunsen-Ges. Phys. Chem.* **1988**, *92*, 273.

(16) Klee, S.; Gericke, K.-H.; Comes, F. J. *Ber. Bunsen-Ges. Phys. Chem.* **1988**, *92*, 429.

(17) Brouard, M.; Martinez, M. T.; O'Mahoney, J.; Simons, J. P. *Mol. Phys.* **1990**, *69*, 65.

(18) Wayne, R. P. *Chemistry of Atmospheres*, 2nd ed; Oxford University Press: New York, 1993; p 90.

(19) Schiffman, A.; Nelson, D. D.; Nesbitt, D. J. *J. Chem. Phys.* **1993**, *98*, 6935.

(20) Bohn, B.; Zetzsch, C. *J. Phys. Chem. A* **1997**, *101*, 1488.

(21) Kuo, Y.-P.; Wann, G.-H.; Lee, Y. P. *J. Chem. Phys.* **1993**, *99*, 3372.

(22) Huber, K. P., Herzberg, G., Eds. *Molecular Spectra and Molecular Structure IV. Constants of Diatomic Molecules*; Van Nostrand Reinhold: New York, 1979; p 508.

(23) Tinti, N. D. S. *J. Chem. Phys.* **1968**, *48*, 1459.

(24) Aquista N.; Schoen, L. J.; Lide, D. L., Jr. *J. Chem. Phys.* **1968**, *48*, 1534.

(25) Suzer, S.; Andrews, L. *J. Chem. Phys.* **1988**, *88*, 916.

(26) Cheng, M. B.-M.; Lee, Y.-P.; Ogilvie, J. F. *Chem. Phys. Lett.* **1988**, *151*, 109.

(27) Goodman, J.; Brus, L. E. *J. Chem. Phys.* **1977**, *67*, 4858.

(28) Khriachtchev, L.; Pettersson, M.; Tuominen, S.; Räsänen, M. *J. Chem. Phys.* **1997**, *107*, 7252.

(29) Gaussian 94, Revision B.1: Frisch, M. J.; Trucks, G. W.; Schlegel, H. B.; Gill, P. M. W.; Johnson, B. G.; Robb, M. A.; Cheeseman, J. R.; Keith, T.; Petersson, G. A.; Montgomery, J. A.; Raghavachari, K.; Al-Laham, M. A.; Zakrzewski, V. G.; Ortiz, J. V.; Foresman, J. B.; Cioslowski, J.; Stefanov, B. B.; Nanayakkara, A.; Challacombe, M.; Peng, C. Y.; Ayala, P. Y.; Chen, W.; Wong, M. W.; Andres, J. L.; Replogle, E. S.; Gomperts, R.; Martin, R. L.; Fox, D. J.; Binkley, J. S.; Defrees, D. J.; Baker, J.; Stewart, J. P.; Head-Gordon, M.; Gonzalez, C.; Pople, J. A. Gaussian, Inc., Pittsburgh, PA, 1995.

(30) Lundell, J. *J. Phys. Chem.* **1995**, *99*, 14290.

(31) Boys, S. F.; Bernardi, F. *Mol. Phys.* **1970**, *19*, 553.

(32) Lundell, J. Ph.D. Thesis, University of Helsinki, 1995.

(33) Sadlej J.; Buch, V. *J. Chem. Phys.* **1994**, *100*, 4272.

(34) Yaron, D.; Peterson, K. I.; Zolandz, D.; Klemperer, W.; Lovas, F. J.; Suenram, R. D. *J. Chem. Phys.* **1990**, *92*, 7095.

(35) Lundell, J.; Räsänen, M. *J. Phys. Chem.* **1995**, *99*, 14301.

(36) Pimentel, G. C.; McLellan, A. C. *The Hydrogen Bond*; W.H. Freeman & Co.: San Francisco, 1960.

(37) Pettersson, M.; Tuominen, S.; Räsänen, M. *J. Phys. Chem. A* **1997**, *101*, 1166.

(38) Lu, C.-S.; Hughes, E. W.; Giguère, P. A. *J. Am. Chem. Soc.* **1941**, *63*, 1507.

(39) Lannon, J. A.; Verderame, F. D.; Anderson, R. W., Jr. *J. Chem. Phys.* **1971**, *54*, 2212.

(40) (a) Ayers, G. P.; Pullin, A. D. E. *Chem. Phys. Lett.* **1974**, *29*, 609. (b) Ayers, G. P.; Pullin, A. D. E. *Spectrochim. Acta* **1976**, *32A*, 1641. (c) Engdahl, A.; Nelander, B. *J. Mol. Struct.* **1989**, *193*, 101. (d) Ayers, G. P.; Pullin, A. D. E. *Spectrochim. Acta* **1976**, *32A*, 1629, 1695. (e) Bentwood, R. M.; Barnes, A. J.; Orville-Thomas, W. J. *J. Mol. Spectrosc.* **1980**, *84*, 391.

(41) Engdahl, A.; Nelander, B. *J. Chem. Phys.* **1987**, *86*, 1819.

(42) Engdahl, A.; Nelander, B. *Chem. Phys.* **1985**, *100*, 273.

(43) (a) Milligan, D. E.; Jacox, M. E. *J. Chem. Phys.* **1963**, *38*, 2627. (b) Jacox, M. E.; Milligan, D. E. *J. Mol. Struct.* **1972**, *42*, 495. (c) Smith, D. W.; Andrews, L. *J. Chem. Phys.* **1972**, *56*, 4433.

(44) Nelander, B. *J. Phys. Chem. A* **1997**, *101*, 9092.

(45) Schriver, L.; Barreau, C.; Schriver, A. *Chem. Phys.* **1990**, *140*, 429.

(46) Lawrence, W. G.; Apkarian, V. A. *J. Chem. Phys.* **1992,** *97*, 2229.